

Recent Rates of Carbon Accumulation in Montane Fens of Yosemite National Park, California, U.S.A.

Authors: Drexler, Judith Z., Fuller, Christopher C., Orlando, James, and Moore, Peggy E.

Source: Arctic, Antarctic, and Alpine Research, 47(4) : 657-669

Published By: Institute of Arctic and Alpine Research (INSTAAR), University of Colorado

URL: <https://doi.org/10.1657/AAAR0015-002>

BioOne Complete (complete.BioOne.org) is a full-text database of 200 subscribed and open-access titles in the biological, ecological, and environmental sciences published by nonprofit societies, associations, museums, institutions, and presses.

Your use of this PDF, the BioOne Complete website, and all posted and associated content indicates your acceptance of BioOne's Terms of Use, available at www.bioone.org/terms-of-use.

Usage of BioOne Complete content is strictly limited to personal, educational, and non - commercial use. Commercial inquiries or rights and permissions requests should be directed to the individual publisher as copyright holder.

BioOne sees sustainable scholarly publishing as an inherently collaborative enterprise connecting authors, nonprofit publishers, academic institutions, research libraries, and research funders in the common goal of maximizing access to critical research.

Recent rates of carbon accumulation in montane fens of Yosemite National Park, California, U.S.A.

Judith Z. Drexler^{1,4}

Christopher C. Fuller²

James Orlando¹ and

Peggy E. Moore³

¹U.S. Geological Survey, California Water Science Center, 6000 J Street, Placer Hall, Sacramento, California, U.S.A.

²U.S. Geological Survey, National Research Program, 345 Middlefield Road, MS465, Menlo Park, California 94025, U.S.A.

³U.S. Geological Survey, Western Ecological Research Center, Yosemite Field Station, 5083 Foresta Road, El Portal, California 95318, U.S.A.

⁴Corresponding author:
jdrexler@usgs.gov

Abstract

Little is known about recent rates of carbon storage in montane peatlands, particularly in the western United States. Here we report on recent rates of carbon accumulation (past 50 to 100 years) in montane groundwater-fed peatlands (fens) of Yosemite National Park in central California, U.S.A. Peat cores were collected at three sites ranging in elevation from 2070 to 2500 m. Core sections were analyzed for bulk density, % organic carbon, and ²¹⁰Pb activities for dating purposes. Organic carbon densities ranged from 0.026 to 0.065 g C cm⁻³. Mean vertical accretion rates estimated using ²¹⁰Pb over the 50-year period from ~1960 to 2011 and the 100-year period from ~1910 to 2011 were 0.28 (standard deviation = ±0.09) and 0.18 (±0.04) cm yr⁻¹, respectively. Mean carbon accumulation rates over the 50- and 100-year periods were 95.4 (±25.4) and 74.7 (±17.2) g C m⁻² yr⁻¹, respectively. Such rates are similar to recent rates of carbon accumulation in rich fens in western Canada, but more studies are needed to definitively establish both the similarities and differences in peat formation between boreal and temperate montane fens.

DOI: <http://dx.doi.org/10.1657/AAAR0015-002>

Introduction

Mountain ranges in the western United States, including the Rockies, the Sierra Nevada, and the Cascades, are replete with meadows. Of these meadows, some rely solely on surface water and snowpack for sustenance, while others receive groundwater flows in addition to any surface water inputs (Benedict, 1983; Bartolome et al., 1990; Cooper and Wolf, 2006). Meadows that receive groundwater inputs are termed *fens* and are the wettest meadow type. Because of their hydrology, fens are the only meadows that (1) remain wet throughout the dry summer season, providing critical refugia for birds, mammals, and amphibians (including the federally threatened Yosemite toad; Department of Interior, Fish and Wildlife Service, 2014) and (2) accrete highly organic soils (peat) at least 40 cm thick but often much deeper (Bartolome et al., 1990; Cooper and Wolf, 2006; Drexler et al., 2013a).

In order for peat to form in fens and other peatlands, there must be a positive water balance and rates of primary production and organic accumulation must be greater than decomposition (Moore and Bellamy, 1974; Clymo, 1983). In a particular peatland, the net balance between production and decomposition hinges on plant community composition, the soil and bedrock properties, and the climatic and hydrologic regime (Moore and Bellamy, 1974; Clymo, 1983; Bridgman et al., 2001). Through peat formation and its long-term storage, montane fens as well as other peatlands have the capability to store carbon for thousands of years (Moore and Bellamy, 1974; Clymo, 1983). This innate ability of peatlands has recently attracted considerable attention as land managers look for ways for reducing carbon pollution while also reaping co-benefits such as improvements in habitat value (Olander et al., 2012; Crooks et al., 2014; Department of Interior, Fish and Wildlife Service, 2014). As an example, the state of California is currently considering all options for biological carbon sequestration to satisfy the carbon reduction requirements that will soon be mandated under the Global Warming Solutions Act of 2006 (California Environmental Protection Agency, 2014).

Despite previous research on fen carbon cycling in the western United States (e.g., West et al., 1999; Wickland et al., 2001; Chimner and Cooper, 2002, 2003), little is known about recent rates (past 50 to 100 years) of carbon accumulation in these systems. Such estimates are important to assess the potential for using fen restoration to reduce carbon pollution. In this paper, we provide estimates of recent rates of carbon accumulation in three fens in Yosemite National Park, located in central California, U.S.A. In addition, we compare our results to the greater literature in order to better understand how our Yosemite sites fit into the broader picture of recent carbon accumulation in fens.

Methods

STUDY AREA

Yosemite National Park covers an area of 3026 km² and is located in central California in the Sierra Nevada range (Fig. 1). The entire Sierra Nevada contains an estimated 17,000 meadows, which cover an area of approximately 77,660 ha (Fryjoff-Hung and Viers, 2012). The park was established in 1890 and spans elevations ranging from about 600 to 4000 m with over 95% designated as wilderness (National Park Service, 2014). Climate in the park is Mediterranean with warm, dry summers and cold, moist winters. Precipitation falls mainly as snow and occurs mostly between October and March. The fens included in this study all receive steady groundwater flows via springs or seeps and are situated at elevations ranging from upper montane forest, which begins at ~1800 m to subalpine forest, which begins at ~2450 m. Study sites include Drosera Fen (DF, 5.03 ha, 2080 m in elevation above mean sea level [MSL]), Mono Meadow North (MMN, 3.4 ha, 2134 m MSL), and Porcupine Fen (PF, 0.98 ha, 2500 m MSL) (Fig. 1). The annual mean minimum temperature at MMN, which is the mid-elevation site, was 4.97 °C, mean maximum temperature was 17.77 °C, and mean annual precipitation was

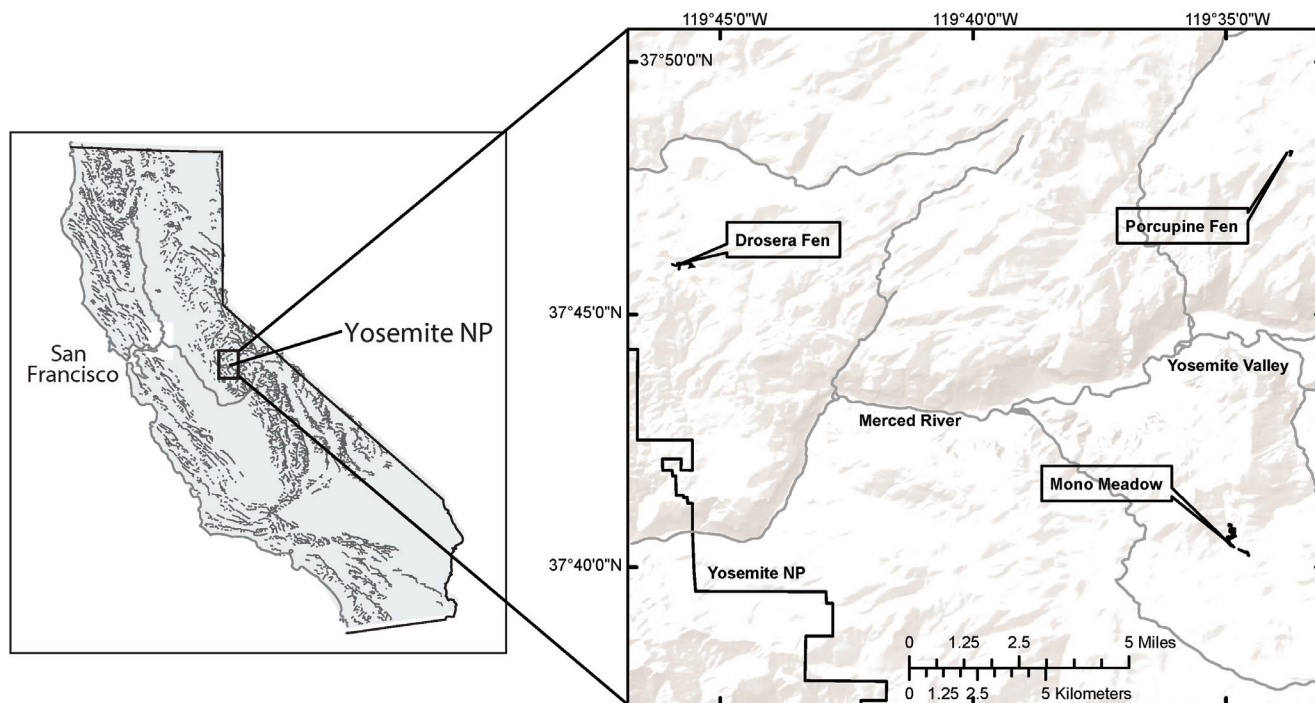


FIGURE 1. Site map showing location of Yosemite National Park in California, U.S.A., and the three Yosemite fen sites.

106.5 cm between 1971 and 2000 (Western Regional Climate Center, 2014). The freeze-free period at Yosemite National Park Headquarters, which is at an elevation of 1200 m, ranges from 130 to 222 days (mean = 176 days, National Oceanic and Atmospheric Administration, 2014). Because the fens are all situated at least 800 m higher than this, the actual freeze-free period at the sites is likely shorter.

The flora of Yosemite fens is highly diverse. Drosera Fen contains a diverse assemblage of forbs/herbs (e.g., *Drosera rotundifolia*

L., *Mimulus primuloides* Benth.), graminoids (e.g., *Carex vesicaria* L., *Carex echinata* Murray ssp. *echinata*) and bryophytes (*Philonotis tomentella* Molendo in Lorentz, and *Sphagnum subsecundum* Nees in Sturm are most common), with no species having greater than 10% cover (all plant community composition data from National Park Service, unpublished data; all nomenclature follows Baldwin et al., 2012, for vascular plants and Wilson, 2013, for bryophytes). Mono Meadow North contains three widely distributed graminoids, *Muhlenbergia filiformis* (Thurb. ex S. Watson) Rydb. (40% cover), *Juncus oxymiris* Engelm (22% cover), and *Carex utriculata* Boott (20% cover). *Sphagnum subsecundum* Nees and *Philonotis tomentella* Molendo in Lorentz each cover over 20% of the coring site. Lastly, Porcupine Fen, similar to Drosera Fen, has great plant diversity with no one species having greater than 7% cover. Graminoids include *Carex utriculata* Boott, *Eleocharis quinqueflora* (Hartmann) O. Schwarz, and *Juncus nevadensis* S. Watson, and bryophytes include *Philonotis* sp. Bridel, *Sphagnum subsecundum* Nees, and *Warnstorfia exannulata* (Schimper) Loeske.

PEAT CORING

Three cores ~50 cm deep were collected in each of the three fen sites in October of 2011. Cores were collected with a Hargis piston corer (Hargis and Twilley, 1994), which minimizes compaction of the peat profile. After collection, cores were sealed airtight at both ends within their acrylic collection tubes, laid horizontally on ice for transport, and stored under refrigeration at the U.S. Geological Survey laboratories in Sacramento, California, U.S.A., until processing.

LABORATORY ANALYSES

All peat cores were processed within 6 weeks of collection. Cores were cut into 2 cm sections, weighed wet, and dried at 80

TABLE 1

Basic characteristics of the top 30 cm (15 sections) of each peat core. Standard deviations ± are shown in parentheses.

Yosemite cores	Mean bulk density (g cm ⁻³)	Mean organic carbon (%)	Mean organic carbon density (g C cm ⁻³)
DF W2	0.10 (0.06)	39.1 (7.4)	0.038 (0.014)
DF M1	0.06 (0.01)	43.6 (1.7)	0.026 (0.004)
DF E3	0.12 (0.08)	40.2 (11.1)	0.043 (0.021)
MMN S3	0.12 (0.04)	32.2 (4.8)	0.037 (0.018)
MMN NE2	0.11 (0.04)	38.6 (3.2)	0.042 (0.015)
MMN NE1	0.14 (0.04)	33.6 (4.0)	0.046 (0.012)
PF 3S	0.18 (0.03)	36.5 (3.7)	0.065 (0.008)
PF 2W	0.18 (0.10)	35.2 (7.4)	0.056 (0.009)
PF 1N	0.15 (0.05)	39.1 (2.7)	0.060 (0.018)
Overall means	0.13 (0.04)	37.6 (3.5)	0.046 (0.012)

°C until reaching a constant dry weight. Dry bulk density was determined using the dry weight of each section of soil and the volume of the core section. Samples were then ground to pass through a 2 mm sieve. Total % carbon and % organic carbon were determined using a Perkin Elmer CHNS/O elemental analyzer (Perkin Elmer Corporation, Waltham, Massachusetts, U.S.A.) according to a modified version of U.S. Environmental Protection Agency Method 440.0 (Zimmerman et al., 2007). For % organic carbon analyses, samples were first exposed to concentrated hydrochloric acid (HCl) fumes in a desiccator for 24 h to remove inorganic carbon. The instrument was calibrated with blanks and acetanilide standards before use. Blanks, replicates, and standards were analyzed every 10 samples to assess instrument stability. Replicate samples were re-analyzed if the relative percentage difference between the two replicates was greater than 20%. Method detection limit for carbon was 0.01%.

Subsections of all the cores were analyzed at the U.S. Geological Survey in Menlo Park, California, for ^{137}Cs , ^{210}Pb , and ^{226}Ra to assign dates to core profiles. Activities of total ^{210}Pb , ^{226}Ra , and ^{137}Cs were measured simultaneously by gamma spectrometry as described in Baskaran and Naidu (1995), Fuller et al. (1999), and Van Metre et al. (2004). Subsamples of dried sediment samples were counted using a high-resolution intrinsic germanium well detector gamma spectrometer. Samples were placed in the detector borehole or well which provides near 4π counting geometry. Sediment samples were sealed in 7 mL polyethylene scintillation vials. The supported ^{210}Pb activity, defined by the ^{226}Ra activity, was determined on each interval from the 352 keV and 609 keV gamma emission lines of the short-lived daughters ^{214}Pb and ^{214}Bi daughters of ^{226}Ra , respectively. Self-absorption of the ^{210}Pb 46 keV gamma emission line was accounted for using an attenuation factor calculated from an empirical relationship between self-absorption and bulk density developed for this geometry based on the method of Cutchall et al. (1983). Additional information regarding standards, random counting errors, and quality assurance/quality control can be found in Drexler et al. (2013b).

Dating by ^{210}Pb and ^{137}Cs has long been used for lake sediments and wetland soils (Armentano and Woodwell, 1975; Lynch et al., 1989; Appleby et al., 1997). The isotope ^{137}Cs , which does not occur naturally, is deposited on the land surface as fallout from nuclear weapons testing and power plant accidents. A maximum or peak in ^{137}Cs activity corresponding to 1963 can usually be clearly identified in a soil profile. However, in this study, subsurface maxima in ^{137}Cs formed broad peaks, were found at variable depths within a site, and, in some profiles, occurred near the peat surface. Such results indicate mobility of ^{137}Cs in the substrate, negating its usefulness as a dating tool. For this reason, we used solely ^{210}Pb dating in this study. ^{210}Pb is a natural isotope of Pb with a half-life of 22.3 years. The total ^{210}Pb pool in soil consists of two parts: (1) a supported ^{210}Pb component produced within the soil via radioactive decay of ^{222}Rn that never diffused to the atmosphere and (2) an unsupported or excess ^{210}Pb component derived from ^{222}Rn that first diffused from continental air masses into the atmosphere and then decayed to ^{210}Pb and deposited on the land surface.

The age-depth relationship in all cores was estimated using the constant rate of supply (CRS) model (Appleby and Oldfield, 1978; Robbins, 1978; Appleby and Oldfield, 1983), and uncertainty analysis of age was conducted following Van Metre and Fuller (2009). The CRS model assumes a constant rate of input of unsupported ^{210}Pb activity per gram to the accreting sediment

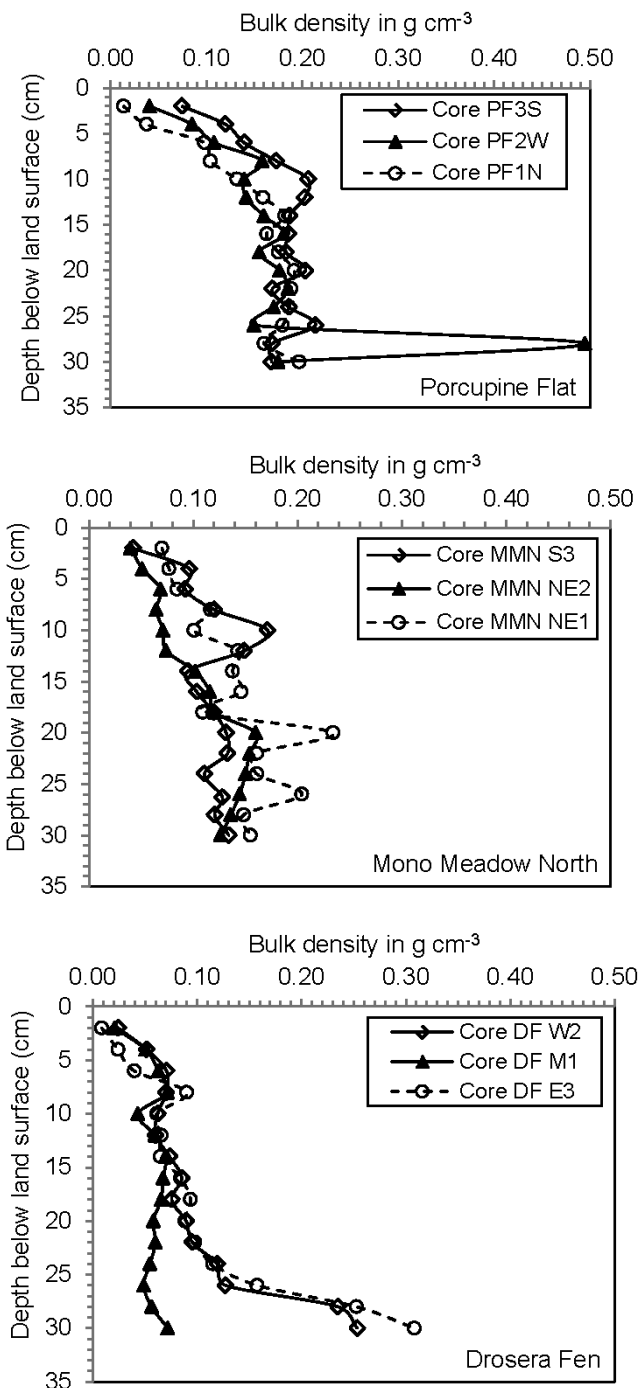


FIGURE 2. Bulk density of each 2 cm section in the top 30 cm of peat cores collected at Porcupine Fen (PF), Mono Meadow North (MMN), and Drosera Fen (DF).

or soil surface to account for temporal variations in accumulation rates. The method determines a mass accumulation rate (MAR) for each core interval by mass balance (in units of $\text{g cm}^{-2}\text{yr}^{-1}$) and depends on measurement of the entire core profile of unsupported ^{210}Pb . The CRS has been successfully applied to fens and bogs in numerous studies (Turetsky et al., 2004; Bauer et al., 2009).

Uncertainty in CRS dates was estimated following the approach outlined in Van Metre and Fuller (2009) to determine the age range that can be dated reliably. The uncertainty in CRS dates

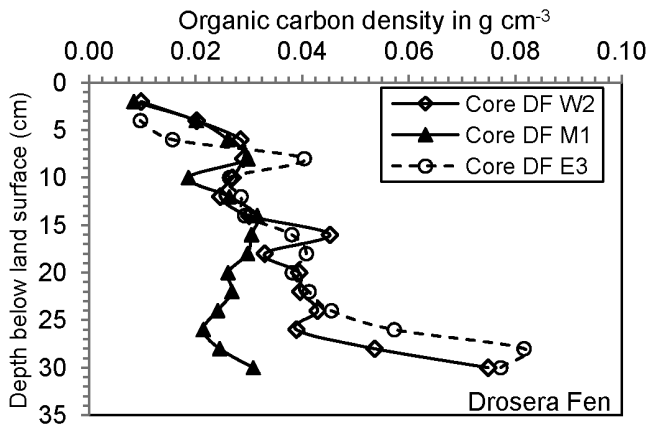
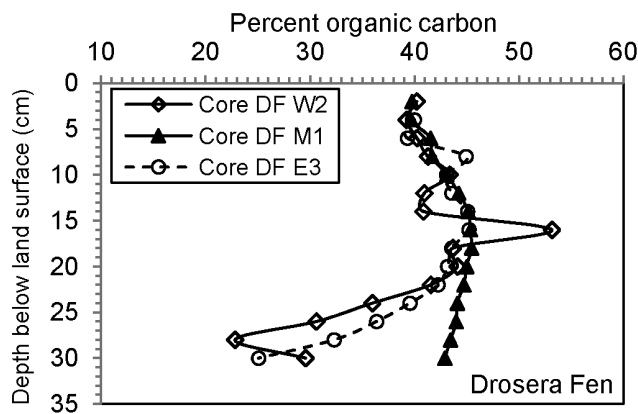
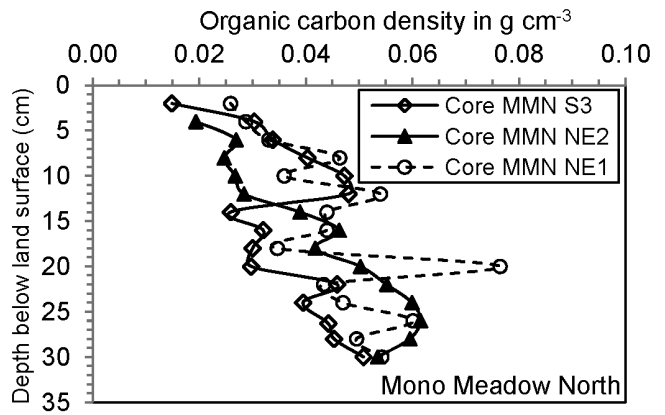
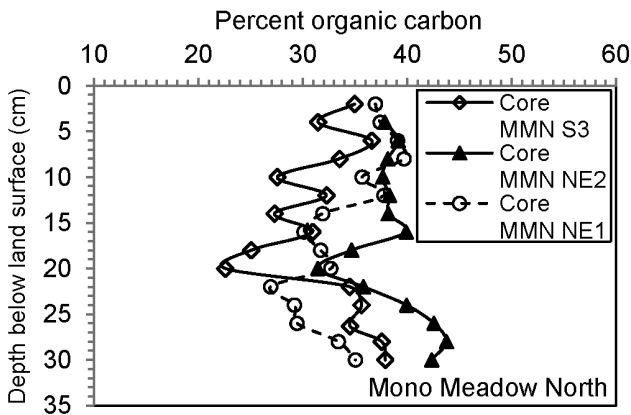
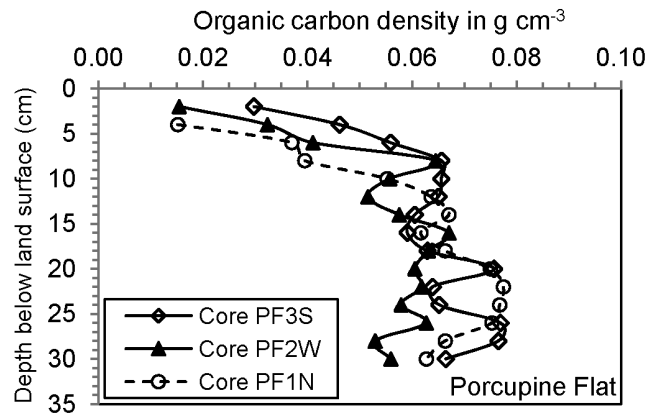
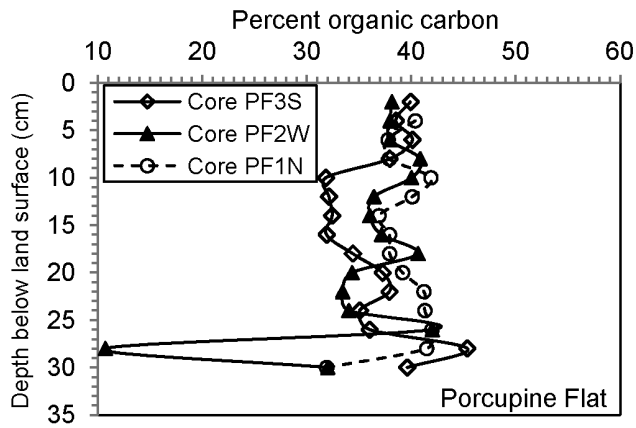


FIGURE 3. Percent organic carbon in each 2 cm section in the top 30 cm of peat cores collected at PF, MMN, and DF.

FIGURE 4. Organic carbon density of each 2 cm section in the top 30 cm of peat cores collected at PF, MMN, and DF.

is calculated by propagating measurement error in the unsupported ^{210}Pb activity through the CRS model calculations. Measurement error in the unsupported ^{210}Pb activity increases with depth and age as the total ^{210}Pb approaches the supported activity. As a result, the uncertainty in CRS model dates increases downward from the surface ultimately to a point where the error in the estimated age is greater than the difference in age between adjacent intervals (Turetsky et al., 2004; MacKenzie et al., 2011). We consider dates of intervals that exceed this level of uncertainty as unreliable and limit dating to intervals with younger ages, typically less than 100 years, which is consistent with other studies (Bricker-Urso et al.,

1989; Thomas and Ridd, 2004; Van Metre and Fuller, 2009; MacKenzie et al., 2011).

The age-depth profiles in conjunction with % organic carbon, bulk density, and section thickness were used to estimate fen vertical accretion and carbon accumulation rates. Vertical accretion rates for each section were determined by dividing the thickness of each section by the age interval of the section (age top – age bottom). Carbon sequestration rates for each section were determined by multiplying the % organic carbon content by the bulk density and dividing by the age interval of the section. Because vertical accretion and carbon accumulation rates were specifically deter-

TABLE 2

Mean vertical accretion (VA) and organic carbon accumulation (CA) rates over ~50 and ~100 years in the Yosemite fens. Standard deviations are shown in parentheses.

Core	VA ₋₁₉₆₀₋₂₀₁₀ (cm yr ⁻¹)	VA ₋₁₉₁₀₋₂₀₁₁ (cm yr ⁻¹)	VA ₋₁₉₆₀₋₂₀₁₀ / VA ₋₁₉₁₀₋₂₀₁₁	CA ₋₁₉₆₀₋₂₀₁₀ (g C m ⁻² yr ⁻¹)	CA ₋₁₉₁₀₋₂₀₁₁ (g C m ⁻² yr ⁻¹)	CA ₋₁₉₆₀₋₂₀₁₀ / CA ₋₁₉₁₀₋₂₀₁₁
DF 2W	0.39 (0.15)	0.21 (0.18)	1.86	118 (27)	72.8 (41.5)	1.62
DF3E	0.35 (0.25)	0.21 (0.27)	1.67	111 (43)	77.2 (51.0)	1.44
MMN NE2	0.28 (0.16)	0.16 (0.16)	1.75	67.3 (22.0)	54.6 (27.9)	1.23
MMN NE1	0.28 (0.13)	0.21 (0.13)	1.31	113 (28)	92.3 (38.3)	1.22
MMN S	0.32 (0.20)	0.23 (0.20)	1.39	120 (35)	99.8 (41.2)	1.20
PF 3S	0.16 (0.02)	0.13 (0.04)	1.23	75.4 (9.8)	71.8 (12.5)	1.05
PF 2W	0.17 (0.12)	0.12 (0.11)	1.42	63.4 (4.3)	54.1 (12.4)	1.17
Overall means	0.28 (0.09)	0.18 (0.04)	1.52	95.4 (25.4)	74.7 (17.2)	1.28

mined for each core section, we calculated time-weighted arithmetic means of these parameters (Drexler et al., 2013b). Vertical accretion and carbon accumulation rates were determined over the past ~50 as well as ~100 years.

Results

Bulk density, % organic carbon, total ²¹⁰Pb activity, ²²⁶Ra activity, and excess ²¹⁰Pb activity, and corresponding error estimates are provided for each 2-cm core section in Appendix Table A1. ²¹⁰Pb dating was successful for all but two cores, DF M1 and PF 1N (see Appendix for explanations regarding exclusion of these cores from the analysis). Mean peat characteristics for each core are shown in Table 1.

Bulk density of peat in each of the three sites generally increased with increasing depth; however, the patterns within sites were somewhat different (Fig. 2). At PF, decreases in bulk density toward the surface were similar among the three profiles, whereas at MMN, the bulk density values had high variability. In one MMN core (NE2), bulk density actually decreased from 20 to 30 cm of depth. At DF, bulk density increased only slightly for DF M1. The other two DF cores had large increases in bulk density from 25 to 30 cm. The mean bulk density of all Yosemite peat cores was 0.13 g cm⁻³ (sd = ±0.06). A single factor ANOVA comparing bulk densities across sites using core means was significant ($p = 0.013$). Post hoc, pairwise comparisons showed that bulk density was significantly greater at the highest elevation site (PF) than the lowest elevation site (DF) ($p = 0.014$, Bonferroni test).

The % organic carbon content at the three sites generally ranged from 23% to 53% (Fig. 3). At PF, most organic carbon values ranged between 31% and 45%; however, one outlier in core PF 2W had an organic carbon content of 11% and a correspondingly high bulk density value of 0.49 g cm⁻³ (Fig. 2), indicating that a large component of inorganic sediment was found in this interval. At DF, cores M1 and E3 were very similar in % organic carbon until 16 cm of depth. Deeper in the core profile (20–28 cm), cores W2 and E3 were quite similar (Fig. 3). Core M1 had very little change with depth (range = ~40% to 45% organic carbon). A single factor ANOVA comparing % organic carbon across sites using core means showed no significant differences between sites ($p = 0.071$).

Organic carbon density ([bulk density] × [% organic carbon content]) spanned a full order of magnitude from 0.008 to 0.08 g C m⁻³ at all three sites (Fig. 4). Values generally increased with depth, but all sites had considerable variability. A single factor ANOVA comparing organic carbon density across sites using core means showed a significant difference between sites ($p = 0.007$). Post hoc, pairwise comparisons revealed that the highest elevation site (PF) had a significantly higher organic carbon density than the lowest elevation site (DF) ($p = 0.007$).

Mean vertical accretion and carbon accumulation rates were determined for all cores that could be dated over the past ~50 (ca. 1960–2011) and ~100 years (ca. 1910–2011) (Table 2). For all sites, mean vertical accretion rates during the 50- and 100-year periods were 0.28 cm yr⁻¹ and 0.18 cm yr⁻¹, respectively. Mean carbon accumulation rates for all sites during the 50- and 100-year period were 95 g C m⁻² yr⁻¹ and 75 g C m⁻² yr⁻¹, respectively. Over the past 100 years, the vertical accretion rates, but not the carbon accumulation rates, had a strong linear relationship with fen elevation (Figs. 5 and 6).

Discussion

Several important observations can be made about how Yosemite peats compare to peat in other fen systems. The bulk density of Yosemite peats (range of core means in the top 30 cm = 0.060 to 0.179 g cm⁻³) is quite similar to the range of values reported in Yu (2006) for fens in subalpine, montane forests, and boreal forests of Alberta, Canada (Table 3), even though the values from the Alberta fens are for the entire peat mass. In contrast, Adkinson et al. (2011) and Vitt et al. (2009) found substantially lower values in fens in northern and central Alberta, Canada (Table 3). The relatively high mean bulk density and overall variability with depth in the Yosemite peats (Fig. 2) likely stem from incorporation of inorganic sediment from the surrounding montane landscape into the peat (Cooper et al., 2012).

The % organic carbon content of Yosemite peats (mean C content in the top 30 cm = 37.6%; Table 1) is lower than the 50% or higher values for the top 1 m of peat cited in a review of northern and subarctic boreal peatlands by Yu (2012). The range of mean values for % organic content in the Yosemite cores (33.6% to 43.6%) fits well within the range found by Cooper and Wolf (2006) for Sierra Nevada fens and is higher than that of Rocky Mountain

TABLE 3

Peat characteristics and recent rates (50 to 100 years) of carbon accumulation in montane and boreal fens.

Fen type	Location; elevation (for montane sites)	Bulk density (g cm ⁻³)	% organic carbon	Carbon accumulation (g C m ⁻² yr ⁻¹ ; method)	Reference
Three temperate montane fens	Yosemite National Park, California, U.S.A.; 2080 to 2500 m	0.06 to 0.179 (range of core means)	33.6% to 43.6% (range of core means)	63 to 120 g C m ⁻² yr ⁻¹ (50-year period) and 54 to 100 g C m ⁻² yr ⁻¹ (100-year period); ²¹⁰ Pb	This paper
182 temperate montane fens	Rocky Mountains, Colorado, U.S.A.; 2532 to 3832 m	NA	30% (mean of all sites using samples from 30 to 40 cm depth interval)	NA	Chimner et al. (2010)
99 temperate montane fens	Sierra Nevada, California, U.S.A.; ~1300 to 3200 m	NA	~25% to 45% (range approximated from Fig. 11#)	NA	Cooper and Wolf (2006)
Two boreal fen-to-spruce forest transects	Central Saskatchewan, Canada	NA	NA	106 to 156 (past 50 years); ²¹⁰ Pb	Bauer et al. (2009)
Boreal poor fen and boreal extremely rich fen	Northern Alberta, Canada	0.046 and 0.083 (core means)	47% and 48% (core means)	160 and 78 over 62 and 88.5 years, respectively; ²¹⁰ Pb	Adkinson et al. (2011)
Three boreal rich fens	Central Alberta, Canada	0.09 to 0.12, maximum values of cores (range = ~0.03–0.12; Fig. 3)	47%	67 to 126 over 50 years; ²¹⁰ Pb	Vitt et al. (2009)
Five boreal rich fens and one boreal poor fen	Alberta, Canada	0.068 to 0.176 (core means)	NA	NA	Yu (2006)
Three temperate montane fens	Mount Changbai, northeast China (near China/N. Korea border); 1280 m	NA	32% to 40% (core means)	ID	Wang et al. (2012)

NA = not available.

ID = insufficient data provided on methodology to include results.

*Assuming 0.5 * % Organic Matter = % Organic Carbon.

fens (Chimner et al., 2010; Table 3). Yosemite peats appear to have a lower carbon content than rich fens in Alberta (Table 3). In addition, Yosemite peats have lower organic carbon densities (0.026 to 0.065 [mean = 0.046] g C cm⁻³; Table 1, Fig. 4), than the global mean in the top 1 m of peat of 0.069 g C cm⁻³ for northern boreal and subarctic peatlands (Table 2 in Yu [2012] excluding the very high value [0.113 g C cm⁻³] from Oechel [1989]).

Few estimates are available for recent rates of carbon accumulation in fens. In Table 3, we only included estimates of carbon accumulation rates over the past 100 years, the period for which uncertainty in ²¹⁰Pb dating is generally considered to be acceptable (see methods). This led to the exclusion of some recent papers (e.g., Bao et al., 2011; Wang et al., 2012; Bao et al., 2014) because

(1) the authors used the ²¹⁰Pb approach to date peat well beyond the ~100 year time frame and (2) the authors did not justify their results by including activity data (i.e., supported ²¹⁰Pb, excess ²¹⁰Pb, and ²²⁶Ra with error estimates) and uncertainty analyses for dates attributed to the peat profile.

Recent rates of carbon accumulation in the Yosemite sites ranged from 63 to 120 g C m⁻² yr⁻¹ (mean = 95.4 [± 25.4] g C m⁻² yr⁻²) over the 50-year period from ~1960 to 2011 and 54 to 100 g C m⁻² yr⁻¹ (mean = 74.7 [± 17.2] g C m⁻² yr⁻²) during the 100-year period from ~1910 to 2011 (Table 2). These rates are quite similar to the rates measured in rich fens by Adkinson et al. (2011) and Vitt et al. (2009) in Alberta, Canada, over similar time periods (Table 3). The rates in the Yosemite fens were lower than those

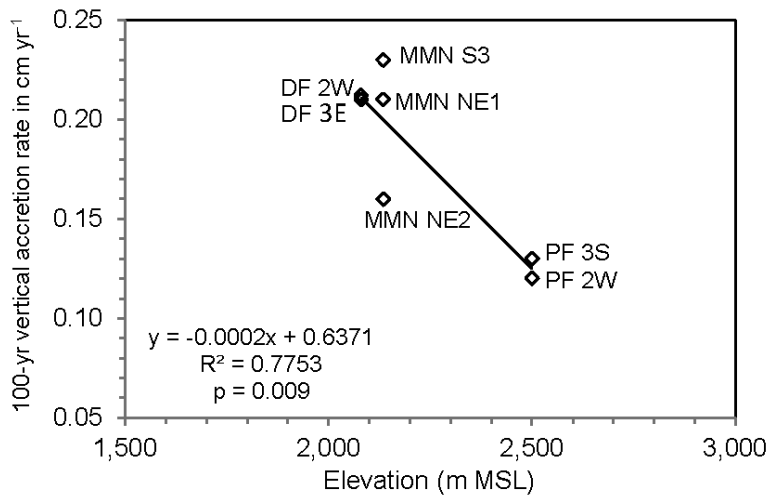


FIGURE 5. Vertical accretion rates over the past ~100 years versus elevation for Yosemite fen sites. A significant inverse linear relationship exists between vertical accretion and elevation.

in a poor fen studied by Adkinson et al. (2011) and the range of rates in the Yosemite fens were lower than the two fen-to-forest transects in central Saskatchewan studied by Bauer et al. (2009) (Table 3).

Mean vertical accretion rates in the Yosemite fens were 0.28 (0.09) and 0.18 (0.04) cm yr⁻¹ during the 50- and 100-year periods, respectively (Table 2). The ratios of the 50-year and 100-year rates ranged from 1.23 to 1.86, demonstrating that major changes, due to processes such as decomposition, consolidation, and compaction, occurred in the peat between the 50 year and 100 year mark (Table 2). Few fen studies are available that include *recent* rates of vertical accretion. Vitt et al. (2009) reported a range of 0.32 to 0.66 cm yr⁻¹ in three rich fens in central Alberta, Canada, over a 50-year period. In the Yosemite fens, vertical accretion rates had an inverse relationship with elevation (Fig. 5). Vertical accretion rates in peatlands typically depend on plant productivity (which is largely controlled by climate and plant community composition), the amount of sediment input, and the rate of decomposition (which is strongly influenced by the elevation of the water table) (Vitt et al., 2009;

Cooper et al., 2012). Without more data on the specific conditions at each site, particularly site hydrology, it is difficult to explain the reason for this pattern. An inverse relationship with elevation was not found for carbon accumulation rates, which were similar across all sites (Fig. 6).

This study demonstrates that Yosemite fens provide the important ecosystem service of carbon storage at rates similar to rich fens in western Canada. However, more studies are needed to understand whether these similarities hold up in a larger sample. In addition, further research is needed to determine whether montane peatlands, similar to several northern bogs and fens (Yu, 2012) have a positive net ecosystem carbon balance (NECB), which is defined as the balance between all sources of carbon inputs and all avenues of carbon loss, including emissions of CO₂ and CH₄ (Chapin et al., 2006). Research on the NECB of montane fens could facilitate entry of fen restoration projects into emerging carbon markets. Such activities may be the financial catalyst needed to achieve better management of montane fens in the western United States, including expansion and improvement of habitat for sensitive species such as the federally threatened Yosemite toad.

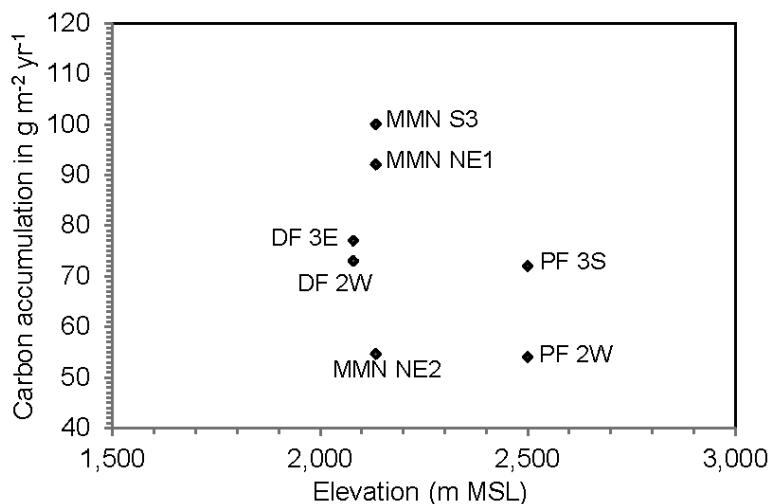


FIGURE 6. Carbon accumulation rates over the past ~100 years versus elevation for Yosemite fen sites. No significant linear relationship was found between carbon sequestration rates at the fens and elevation ($p = 0.11$).

Acknowledgments

This project was funded by U.S. Geological Survey–National Park Service Park Oriented Biological Support Program. We thank Niki Stephanie Nicholas and others at Yosemite National Park for their support of this project. We appreciate receiving background information on Yosemite fens from David Cooper. We are grateful to the anonymous reviewers for offering substantial comments that improved the manuscript.

References Cited

- Adkinson, A. C., Syed, K. H., and Flanagan, L. B., 2011: Contrasting responses of growing season ecosystem CO₂ exchange to variation in temperature and water table depth in two peatlands in northern Alberta, Canada. *Journal of Geophysical Research*, 116: G01004, doi <http://dx.doi.org/10.1029/2010JG001512>.
- Appleby, P. G., and Oldfield, F. R., 1978: The calculation of ²¹⁰Pb dates assuming a constant rate of supply of unsupported ²¹⁰Pb to the sediment. *Catena* (Supplement), 5: 1–8.
- Appleby, P. G., and Oldfield, F. R., 1983: The assessment of ²¹⁰Pb data from sites with varying sediment accumulation rates. *Hydrobiologia*, 103: 29–35.
- Appleby, P. G., Shotyk, W., and Fankhauser, A., 1997: Lead-210 age dating of three peat cores in the Jura Mountains, Switzerland. *Water, Air, and Soil Pollution*, 100: 223–231.
- Armentano, T. M., and Woodwell, G. M., 1975: Sedimentation rates in a Long Island marsh determined by ²¹⁰Pb dating. *Limnology and Oceanography*, 20: 452–456.
- Baldwin B. G., Goldman, D. H., Keil, D. J., Patterson, R., Rosatti, T. J., and Wilken, D. H. (eds.), 2012: *The Jepson Manual: Vascular Plants of California*, Second edition. Berkeley: University of California Press.
- Bao, K., Zhao, H., Xing, W., Lu, X., McLaughlin, N. B., and Wang, G., 2011: Carbon accumulation in temperate wetlands of the Sanjiang Plain, northeast China. *Soil Science Society of America Journal*, 75: 2386–2397.
- Bao, K., Wang, G., Xing, W., and Shen, J., 2014: Accumulation of organic carbon over the past 200 years in alpine peatlands, northeast China. *Environmental Earth Sciences*, doi <http://dx.doi.org/10.1007/s12665-014-3922-1>.
- Bartolome, J. W., Erman, D. C., and Schwarz, C. F., 1990: *Stability and Change in Minerotrophic Peatlands, Sierra Nevada of California and Nevada*. Berkeley, California: Pacific Southwest and Range Experimental Station, Research Paper PSW-198, 1–11.
- Baskaran, M., and Naidu, A. S., 1995: ²¹⁰Pb-derived chronology and the fluxes of ²¹⁰Pb and ¹³⁷Cs isotopes into continental shelf sediments, East Chukchi Sea, Alaskan Arctic. *Geochimica et Cosmochimica Acta*, 59: 4435–4448.
- Bauer, I. E., Bhatti, J. S., Swanston, C., Wieder, R. K., and Preston, C. M., 2009: Organic matter accumulation and community change at the peatland-upland interface: inferences from ¹⁴C and ²¹⁰Pb dated profiles. *Ecosystems*, 12: 636–653.
- Benedict, N. B., 1983: Plant associations of alpine meadows, Sequoia National Park, California. *Arctic and Alpine Research*, 15: 383–396.
- Bricker-Urso, S., Nixon, S. W., Cochran, J. K., Hirschberg, D. J., and Hunt, C., 1989: Accretion rates and sediment accumulation in Rhodes Island salt marshes. *Estuaries*, 12: 300–317.
- Bridgman, S. D., Ping, C.-L., Richardson, J. L., and Updegraff, K., 2001: Soils of northern peatlands: histosols and gelsols. In Richardson, J. L., and Vespraskas, M. J. (eds.) *Wetland Soils: Genesis, Hydrology, Landscapes, and Classification*. Boca Raton, Florida: CRC Press, 343–370.
- California Environmental Protection Agency, 2014: Assembly Bill 32: Global Warming Solutions Act, available online at <http://www.arb.ca.gov/cc/ab32/ab32.htm>.
- Chapin, F. S., III, Woodwell, G. M., Randerson, J. T., Rastetter, E. B., Lovett, G. M., Baldocchi, D. D., Clark, D. A., Harmon, M. E., Schimel, D. S., Valentini, R., Wirth, C., Aber, J. D., Cole, J. J., Goulden, M. L., Harden, J. W., Heimann, M., Howarth, R. W., Matson, P. A., McGuire, A. D., Melillo, J. M., Mooney, H. A., Neff, J. C., Houghton, R. A., Pace, M. L., Ryan, M. G., Running, S. W., Sala, O. E., Schlesinger, W. H., and Schulze, E.-D., 2006: Reconciling carbon-cycle concepts, terminology, and methods. *Ecosystems*, 9: 1041–1050.
- Chimner, R. A., and Cooper, D. J., 2002: Modeling carbon accumulation in Rocky Mountain fens. *Wetlands*, 22: 100–110.
- Chimner, R. A., and Cooper, D. J., 2003: Carbon dynamics of pristine and hydrologically modified fens in the southern Rocky Mountains. *Canadian Journal of Botany*, 81: 477–491.
- Chimner, R. A., Lemly, J. M., and Cooper, D. J., 2010: Mountain fen distribution, types, and restoration priorities, San Juan Mountains, Colorado, USA. *Wetlands*, 30: 763–771.
- Clymo, S., 1983: Peat. In Gore, A. J. P. (ed.), *Ecosystems of the World, Vol. 4A: Mires: Swamp, Bog, Fen, and Moor*. Amsterdam: Elsevier, 159–224.
- Cooper, D. J., and Wolf, E. C., 2006: *Fens of the Sierra Nevada, California*. Albany, California: Final Report to the USDA Forest Service, Southwest Region.
- Cooper, D. J., Chimner, R. A., and Merritt, D. M., 2012: Chapter 22: Western Mountain Wetlands. In Batzer, D. P., and Baldwin, A. H. (eds.), *Wetland Habitats of North America: Ecology and Conservation Concerns*. Berkeley: University of California Press, 313–328.
- Crooks, S., Rybczyk, J., O’Connell, K., Devier, D. L., Poppe, K., and Emmett-Mattox, S., 2014: *Coastal Blue Carbon Opportunity Assessment for the Snohomish Estuary: The Climate Benefits of Estuary Restoration*. Report by Environmental Science Associates, Western Washington University, EarthCorps, and Restore America’s Estuaries, available at http://www.estuaries.org/images/stories/RAEReports/snohomish_report.pdf.
- Cutshall, N. H., Larsen, I. L., and Olsen, C. R., 1983: Direct analysis of ²¹⁰Pb in sediment samples: self-absorption corrections. *Nuclear Instruments and Methods*, 306: 309–312.
- Department of Interior, Fish and Wildlife Service, 2014: Endangered and threatened wildlife and plants; endangered species status for Sierra Nevada yellow-legged frog and northern distinct population segment of the mountain yellow-legged frog, and threatened species status for Yosemite toad. *Federal Register*, 79:82; April 29; 50 CFR Part 17, Docket No. FWS–R8–ES–2012–0100; 4500030113.
- Drexler, J. Z., Knifong, D., Tuil, J., Flint, L., and Flint, A., 2013a: Fens as whole-ecosystem gauges of groundwater recharge under climate change. *Journal of Hydrology*, 481: 22–34.
- Drexler, J. Z., Krauss, K. W., Sasser, M. C., Fuller, C. C., Swarzenski, C. M., Powell, A., Swanson, K. M., and Orlando, J., 2013b: A long-term comparison of carbon sequestration rates in impounded and naturally tidal freshwater marshes along the Lower Waccamaw River, South Carolina. *Wetlands*, 33: 965–974.
- Fryjoff-Hung, A., and Viers, J., 2012: Sierra Nevada multi-source meadow polygons compilation (v 1.0), University of California, Davis, Center for Watershed Sciences, available at <http://meadows.ucdavis.edu/>.
- Fuller, C. C., van Geen, A., Baskaran, M., and Anima, R., 1999: Sediment chronology in San Francisco Bay defined by ²¹⁰Pb, ²³⁴Th, ¹³⁷Cs, and ^{239,240}Pu. *Marine Chemistry*, 64: 7–27.
- Hargis, T. G., and Twilley, R. R., 1994: Improved coring device for measuring soil bulk density in a Louisiana deltaic marsh. *Journal of Sedimentary Research Section A: Sedimentary Petrology and Processes*, 64: 681–683.
- Lynch, J. C., Meriwether, J. R., McKee, B. A., Vera-Herrera, F., and Twilley, R. R., 1989: Recent accretion in mangrove ecosystems of ¹³⁷Cs and ²¹⁰Pb. *Estuaries*, 12: 284–299.
- MacKenzie, A. B., Hardie, S. M. L., Farmer, J. G., Eades, L. J., and Pulford, I. D., 2011: Analytical and sampling constraints in ²¹⁰Pb dating. *Science of the Total Environment*, 409: 1298–1304.
- Moore, P. D., and Bellamy, D. J., 1974: *Peatlands*. New York: Springer-Verlag.

- National Oceanic and Atmospheric Administration, National Climate Data Center, 2014: *Climate Data Online: Freeze/Frost Occurrence Data for California*, available at <http://www.ncdc.noaa.gov/cdo-web/>.
- National Park Service, 2014: *Yosemite National Park, California*, available at <http://www.nps.gov/yose/index.htm>.
- Oechel, W. C., 1989: Nutrient and water flux in a small Arctic watershed: an overview. *Holarctic Ecology*, 12: 229–237.
- Olander, L. P., Cooley, D. M., and Galik, C. S., 2012: The potential role for management of U.S. public lands in greenhouse gas mitigation and climate policy. *Environmental Management*, 49: 523–533.
- Robbins, J. A., 1978: Geochemical and geophysical applications of radioactive lead. In Nriagu, J. O. (ed.), *Biogeochemistry of Lead in the Environment*. Amsterdam: Elsevier Scientific, 285–393.
- Thomas, S., and Ridd, P. V., 2004: Review of methods to measure short time scale sediment accumulation. *Marine Geology*, 207: 95–114.
- Turetsky, M. R., Manning, S. W., and Wieder, R. K., 2004: Dating recent peat deposits. *Wetlands*, 24: 324–356.
- Van Metre, P. C., and Fuller, C. C., 2009: Dual-core mass-balance approach for evaluating mercury and ²¹⁰Pb atmospheric fallout and focusing to lakes. *Environmental Science and Technology*, 43: 26–32.
- Van Metre, P. C., Wilson, J. T., Fuller, C. C., Callender, E., and Mahler, B. J., 2004: Collection, analysis, and age-dating of sediment cores from 56 U.S. lakes and reservoirs sampled by the U.S. Geological Survey, 1992–2001. *U.S. Geological Survey Scientific Investigations*, Report 2004-5184.
- Vitt, D. H., Wieder, R. K., Scott, K. D., and Faller, S., 2009: Decomposition and peat accumulation in rich fens of boreal Alberta, Canada. *Ecosystems*, 12: 360–373.
- Wang, G., Bao, K., Yu, X., Zhao, H., Lin, Q., and Lu, X., 2012: Forms and accumulation of soil P in a subalpine peatland of Mt. Changbai in northeast China. *Catena*, 92: 22–29.
- West, A. E., Brooks, P. D., Fisk, M. C., Smith, L. K., Holland, E. A., Jaeger, C. H., Babcock, S., Lai, R. S., and Schmidt, S. K., 1999: Landscape patterns of CH₄ fluxes in an alpine tundra ecosystem. *Biogeochemistry*, 45: 243–264.
- Western Regional Climate Center, 2014: Historical climate information, available at <http://www.wrcc.dri.edu/index.html> (accessed 22 January 2015).
- Wickland, K. P., Striegl, R. G., Mast, M. A., and Clow, D. W., 2001: Carbon gas exchange at a southern Rocky Mountain wetland, 1996–1998. *Global Biogeochemical Cycles*, 15: 321–335.
- Wilson, P. (ed.), 2013: *California Moss eFlora*, available at http://ucjeps.berkeley.edu/CA_moss_eflora.
- Yu, Z. C., 2006: Holocene carbon accumulation of fen peatlands in boreal western Canada: complex ecosystem response to climate variation and disturbance. *Ecosystems*, 9: 1278–1288.
- Yu, Z. C., 2012: Northern peatland carbon stocks and dynamics: a review. *Biogeosciences*, 9: 4071–4085.
- Zimmerman, C. F., Keefe, C. W., and Bashe, J., 2007: Determination of carbon and nitrogen in sediments and particulates of estuarine/coastal waters using elemental analysis. U.S. Environmental Protection Agency Method 440.0, available at <http://www.caslab.com/EPA-Methods/PDF/EPA-Method-440.pdf>.

MS accepted May 2015

APPENDIX

TABLE A1

Bulk density, % organic carbon, ^{210}Pb , ^{226}Ra , and excess ^{210}Pb data for the top 30 cm or the full ^{210}Pb profile in each core, whichever was greater in depth. Data for cores PF 1N and DF M1 are in italics because the ^{210}Pb data were not used for estimating carbon sequestration or vertical accretion rates. The ^{210}Pb profile for PF 1N had a surface decrease in values, which comprised a large enough time period (~3 years) to reduce the accuracy of estimated dates for the rest of the profile beyond acceptable error. (Core DF E3 also had a decrease in ^{210}Pb at the top of the core, but the effect of the dating on the rest of the core was within acceptable error.) Core DF M1 was omitted from the study because the core did not contain the full profile of excess ^{210}Pb , which is required for application of the CRS model. NA indicates that the data are "not available." Underlined upper sections of cores indicate that surface litter (mainly moss) was the main component of these sections, precluding them from use in calculating vertical accretion and carbon sequestration rates. An asterisk (*) indicates the maximum depth of excess ^{210}Pb .

Depth of section bottom relative to land surface (cm)	Bulk density (g/cm ³)	% Organic carbon	^{210}Pb (dpm g ⁻¹)	±	^{226}Ra (dpm g ⁻¹)	±	Excess ^{210}Pb (dpm g ⁻¹)	±
<i>PF 1N (not used for dating)</i>								
2	0.01	NA	9.52	1.68	0.28	0.48	9.24	1.75
4	0.04	40.4	17.9	1.3	0.98	0.26	16.9	1.3
6	0.10	37.8	30.4	1.5	0.34	0.19	30.0	1.5
8	0.10	37.9	25.6	1.3	0.41	0.17	25.2	1.3
10	0.13	41.9	13.0	0.8	0.65	0.13	12.3	0.8
12	0.16	40.1	5.66	0.52	0.44	0.12	5.22	0.53
14	0.18	36.9	4.12	0.37	0.86	0.09	3.26	0.39
16	0.16	37.9	2.37	0.40	0.82	0.10	1.55	0.42
18	0.18	37.9	1.24	0.36	0.84	0.10	0.41	0.37
20	0.19	39.2	0.99	0.34	0.71	0.09	0.27*	0.35
22	0.19	41.2						
24	0.19	41.3						
26	0.18	42.0						
28	0.16	41.5						
30	0.20	31.9						
<i>PF 2W</i>								
2	0.04	38.1	37.0	2.6	1.31	0.49	35.7	2.6
4	0.09	37.9	25.7	1.6	0.51	0.32	25.2	1.6
6	0.11	38.0	17.7	1.1	0.42	0.21	17.3	1.1
8	0.16	40.9	13.3	1.0	0.57	0.21	12.7	1.0
10	0.14	40.0	8.54	0.70	0.59	0.14	7.95	0.71
12	0.14	36.4	3.98	0.52	1.57	0.13	2.41	0.53
14	0.16	36.0	3.55	0.37	1.13	0.09	2.42	0.38
16	0.18	37.2	1.21	0.26	0.60	0.07	0.61	0.26
18	0.16	40.6	1.35	0.33	0.73	0.09	0.62	0.34
20	0.18	34.3	1.28	0.37	0.91	0.10	0.37	0.38
22	0.19	33.4	1.79	0.38	1.22	0.10	0.56*	0.40
24	0.17	34.0						
26	0.15	42.0						
28	0.50	10.7						
30	0.17	32.0						
<i>PF 3S</i>								
2	0.07	39.9	26.0	2.2	0.49	0.17	25.5	2.2

TABLE A1
Continued

Depth of section bottom relative to land surface (cm)	Bulk density (g/cm ³)	% Organic carbon	²¹⁰ Pb (dpm g ⁻¹)	±	²²⁶ Ra (dpm g ⁻¹)	±	Excess ²¹⁰ Pb (dpm g ⁻¹)	±
4	0.12	38.5	14.5	1.1	0.45	0.08	14.0	1.2
6	0.14	40.1	9.36	0.8	0.19	0.07	9.17	0.76
8	0.17	37.9	5.88	0.53	0.53	0.07	5.35	0.53
10	0.21	31.8	4.53	0.42	1.65	0.07	2.88	0.42
12	0.20	32.1	3.46	0.36	1.28	0.07	2.18	0.36
14	0.19	32.4	1.64	0.22	0.97	0.05	0.66	0.22
16	0.19	31.9	1.42	0.21	0.91	0.05	0.52	0.22
18	0.18	34.4	1.02	0.21	0.77	0.05	0.24	0.22
20	0.20	37.2	1.08	0.16	0.64	0.04	0.44*	0.17
22	0.17	37.9	0.63	0.19	0.52	0.05	0.11	0.19
24	0.19	35.1	1.22	0.20	1.17	0.05	0.06	0.21
26	0.21	36.0	0.97	0.20	0.72	0.05	0.26	0.20
28	0.17	45.4						
30	0.17	39.6						
<i>MMN NE1</i>								
2	0.07	36.9	10.9	0.9	0.32	0.20	10.6	0.9
4	0.08	37.4	10.3	1.0	0.12	0.22	10.2	1.0
6	0.08	39.1	8.85	0.73	0.58	0.17	8.27	0.75
8	0.12	39.7	10.1	0.7	0.61	0.14	9.53	0.69
10	0.10	35.7	6.64	0.68	0.56	0.16	6.09	0.70
12	0.14	37.8	5.84	0.58	0.81	0.13	5.03	0.59
14	0.14	31.9	7.38	0.65	1.56	0.15	5.82	0.67
16	0.15	30.1	4.48	0.51	1.70	0.12	2.78	0.52
18	0.11	31.7	4.25	0.42	1.10	0.10	3.15	0.43
20	0.23	32.7	3.58	0.38	1.51	0.09	2.06	0.39
22	0.16	26.9	3.00	0.40	1.70	0.11	1.30	0.42
24	0.16	29.2	1.83	0.27	1.54	0.07	0.29	0.28
26	0.20	29.5	1.86	0.31	1.54	0.08	0.32	0.32
28	0.15	33.4	1.38	0.25	0.80	0.06	0.58	0.25
30	0.15	35.0	1.38	0.24	0.89	0.06	0.49*	0.25
<i>MMN NE2</i>								
2	0.04	37.8	12.3	1.2	0.56	0.27	11.7	1.3
4	0.05	37.9	12.3	0.8	0.69	0.17	11.6	0.8
6	0.07	39.1	9.10	0.70	0.34	0.16	8.76	0.72
8	0.06	38.1	9.22	0.81	0.74	0.19	8.48	0.84
10	0.07	37.7	9.00	0.75	0.37	0.16	8.63	0.77
12	0.07	38.3	8.35	0.66	0.71	0.14	7.64	0.68
14	0.10	38.2	7.25	0.47	0.60	0.10	6.65	0.48
16	0.12	39.9	5.88	0.56	0.54	0.13	5.33	0.58
18	0.12	34.7	4.05	0.35	1.18	0.08	2.87	0.36
20	0.16	31.4	3.50	0.34	1.43	0.08	2.07	0.35

TABLE A1
Continued

Depth of section bottom relative to land surface (cm)	Bulk density (g/cm ³)	% Organic carbon	²¹⁰ Pb (dpm g ⁻¹)	±	²²⁶ Ra (dpm g ⁻¹)	±	Excess ²¹⁰ Pb (dpm g ⁻¹)	±
22	0.15	35.8	1.89	0.26	1.03	0.06	0.86	0.26
24	0.15	39.9	0.99	0.21	0.76	0.06	0.23*	0.22
26	0.14	42.6	1.00	0.23	0.50	0.06	0.50	0.23
28	0.14	43.8	1.15	0.23	0.64	0.06	0.50	0.24
30	0.13	42.3	1.19	0.25	0.36	0.06	0.83	0.26
<i>MMNS</i>								
2	0.04	35.0	9.71	0.65	0.72	0.13	8.99	0.66
4	0.10	31.5	9.54	0.60	1.02	0.12	8.52	0.61
6	0.09	36.6	8.89	0.77	0.86	0.17	8.04	0.79
8	0.12	33.5	9.00	0.62	1.14	0.13	7.86	0.63
10	0.17	27.6	7.27	0.63	1.36	0.14	5.91	0.64
12	0.15	32.3	5.58	0.45	1.02	0.10	4.56	0.46
14	0.09	27.3	5.67	0.44	0.80	0.10	4.87	0.45
16	0.10	30.9	4.87	0.43	1.15	0.10	3.72	0.44
18	0.12	25.1	4.94	0.46	1.19	0.10	3.74	0.47
20	0.13	22.6	4.40	0.36	1.55	0.08	2.85	0.37
22	0.13	34.5	3.97	0.28	1.00	0.06	2.97	0.28
24	0.11	35.6	2.91	0.28	1.13	0.07	1.77	0.28
26	0.13	34.5	1.88	0.27	0.95	0.07	0.93	0.28
28	0.12	37.6	1.82	0.26	0.89	0.06	0.93	0.26
30	0.13	37.9	1.50	0.25	1.02	0.06	0.48	0.26
32	0.13	40.9	1.34	0.22	0.82	0.06	0.52	0.23
34	0.13	36.8	1.34	0.25	0.71	0.06	0.63*	0.26
<i>DF MI (not used for dating)</i>								
2	0.02	39.7	11.9	0.9	0.32	0.18	11.6	0.9
4	0.05	39.7	15.7	0.8	-0.14	0.13	15.7	0.8
6	0.06	41.5	16.8	1.14	-0.11	0.25	16.8	1.1
8	0.07	41.7	13.0	0.9	0.07	0.20	13.0	0.9
10	0.04	43.1	15.2	1.0	0.13	0.22	15.1	1.1
12	0.06	44.2	15.3	1.1	-0.02	0.24	15.3	1.3
14	0.07	45.1	12.0	1.0	-0.29	0.21	12.0	1.0
16	0.07	45.4	15.0	1.0	0.39	0.20	14.6	1.0
18	0.07	45.4	14.3	1.2	0.12	0.27	14.2	1.2
20	0.06	45.0	12.1	0.9	0.46	0.20	11.6	0.9
22	0.06	44.7	13.5	1.0	0.44	0.23	12.9	1.1
24	0.05	44.1	11.4	1.1	0.41	0.25	10.9	1.1
26	0.05	44.0	10.6	1.1	0.15	0.27	10.4	1.2
28	0.06	43.5	11.2	1.1	1.19	0.27	10.1	1.1
30	0.07	42.9	9.23	1.06	1.47	0.26	7.76	1.09
32	0.07	42.9	8.39	0.89	0.16	0.15	8.23	0.90
34	0.08	41.2	7.48	0.98	0.62	0.20	6.86	1.00

TABLE A1
Continued

Depth of section bottom relative to land surface (cm)	Bulk density (g/cm ³)	% Organic carbon	²¹⁰ Pb (dpm g ⁻¹)	±	²²⁶ Ra (dpm g ⁻¹)	±	Excess ²¹⁰ Pb (dpm g ⁻¹)	±
36	0.08	40.3	7.59	0.97	0.27	0.20	7.33	0.99
38	0.07	43.2	5.79	0.94	0.38	0.21	5.41	0.96
40	0.06	41.3	9.03	1.22	0.70	0.26	8.32	1.25
42	NA	41.6	7.80	1.19	1.05	0.27	6.75	1.22
44	NA	38.3	5.88	0.43	0.64	0.09	5.24	0.44
			7.52	0.90	0.31	0.23	7.20	0.93
<i>DF W2</i>								
2	0.02	40.2	13.2	0.9	0.00	0.18	13.2	0.9
4	0.05	39.2	13.6	0.8	0.31	0.15	13.3	0.8
6	0.07	40.3	9.95	0.88	0.00	0.19	9.95	0.88
8	0.07	41.3	9.01	0.85	0.33	0.20	8.69	0.88
10	0.06	43.4	9.56	0.67	0.30	0.15	9.27	0.69
12	0.06	40.9	9.71	0.80	0.21	0.16	9.50	0.82
14	0.07	40.9	9.25	0.75	0.19	0.42	9.06	0.86
16	0.09	53.1	9.53	0.77	0.09	0.16	9.45	0.78
18	0.08	43.7	6.40	0.59	0.03	0.13	6.37	0.60
20	0.09	44.1	5.41	0.39	0.13	0.08	5.28	0.40
22	0.10	41.6	5.01	0.40	0.28	0.09	4.73	0.41
24	0.12	36.0	4.58	0.31	0.32	0.06	4.26	0.31
26	0.11	30.6	3.67	0.44	1.26	0.09	2.41	0.45
28	0.26	22.8	3.31	0.36	1.76	0.08	1.55	0.37
30	0.25	29.6	2.44	0.29	1.97	0.07	0.47*	0.30
<i>DF E3</i>								
2	0.01	40.0	8.57	3.43	3.07	0.95	5.51	3.55
4	0.02	40.0	15.4	1.3	0.05	0.29	15.4	1.3
6	0.04	39.3	21.1	1.4	0.17	0.26	20.9	1.4
8	0.09	44.9	16.3	1.1	0.00	0.58	16.3	1.3
10	0.06	43.1	18.7	1.1	0.00	0.19	18.7	1.1
12	0.07	43.6	17.5	1.1	0.67	0.19	16.9	1.1
14	0.06	45.1	16.6	1.0	0.27	0.17	16.3	1.0
16	0.08	45.2	21.7	0.9	0.43	0.10	21.2	0.9
18	0.09	43.6	16.9	0.9	0.08	0.15	16.8	0.9
20	0.09	43.2	13.3	0.8	0.53	0.40	12.8	0.9
22	0.10	42.2	11.3	0.6	0.07	0.12	11.2	0.6
24	0.11	39.6	7.59	0.53	0.27	0.11	7.31	0.54
26	0.16	36.4	4.79	0.49	0.46	0.08	4.33	0.50
28	0.25	32.3	2.00	0.27	0.58	0.06	1.42	0.27
30	0.31	25.1	1.13	0.21	0.74	0.05	0.39*	0.21